

Lagrangian Analysis and Forecasting in the Oceans and Coastal Zones

Chad M. Coulliette
Control & Dynamical Systems
and Environmental Engineering Science, 107-81
California Institute of Technology
Pasadena, California 91125
phone: (626) 395-3365 fax: (626) 794-8914 email: chad@caltech.edu

Jerrold E. Marsden
Control & Dynamical Systems, 107-81
Pasadena, California 91125
phone: (626) 395-4176 fax: (626) 794-8914 email: marsden@cds.caltech.edu

Grant Number: N000140110208
<http://www.transport.caltech.edu>

LONG-TERM GOALS

The goal of this research program is to develop a more detailed and systematic understanding of transport and mixing in the oceans and coastal zones. Ultimately, the program will lead to Lagrangian forecasting, that is, the ability to make specific deterministic predictions about the advection and diffusion of passive scalars in the ocean. To accomplish this, it will be necessary to unify several rapidly advancing areas: aspects of dynamical systems theory developed to identify transport barriers and coherent Lagrangian structures, Lagrangian stochastic models of turbulent diffusion, and Eulerian observation data, e.g. sea surface height (SSH) from the TOPEX/Poseidon altimeter for global/regional studies and high frequency (HF) radar for coastal studies.

OBJECTIVES

We endeavor to advance dynamical systems templates and the methodology for applying them to recent observation data of the ocean. In particular, we test a new dynamical system theory based on finite-time Lyapunov exponents for identifying Lagrangian barriers in HF radar data of Monterey Bay and the east coast of Florida which dictate where passive particles, such as contaminants released from Moss Landing, will be advected. We address the specific question of whether a given parcel will remain near the coast indefinitely, or will be advected efficiently away from the coast and into the open ocean where it can be safely dispersed. To explore the Lagrangian complexities present in HF radar data and other measurement data, we are developing a new filtering, interpolation and extrapolation method called Open-boundary Modal Analysis (OMA), which presents a function basis for domains with flow across the boundary. Other filtering methods have been limited in their treatment of open boundary conditions, projecting the data only closed-boundary modes only and then applying an ad hoc zero-order mode to compensate for the open boundary. Last, we explore the use of Lagrangian stochastic models to determine the effect of turbulent diffusion on Lagrangian coherent structures identified through the dynamical systems templates. The unification of our filtering method, dynamical systems templates and Lagrangian stochastic models provides a unique set of tools for

Report Documentation Page			Form Approved OMB No. 0704-0188		
Public reporting burden for the collection of information is estimated to average 1 hour per response, including the time for reviewing instructions, searching existing data sources, gathering and maintaining the data needed, and completing and reviewing the collection of information. Send comments regarding this burden estimate or any other aspect of this collection of information, including suggestions for reducing this burden, to Washington Headquarters Services, Directorate for Information Operations and Reports, 1215 Jefferson Davis Highway, Suite 1204, Arlington VA 22202-4302. Respondents should be aware that notwithstanding any other provision of law, no person shall be subject to a penalty for failing to comply with a collection of information if it does not display a currently valid OMB control number.					
1. REPORT DATE 30 SEP 2002		2. REPORT TYPE		3. DATES COVERED 00-00-2002 to 00-00-2002	
4. TITLE AND SUBTITLE Lagrangian Analysis and Forecasting in the Oceans and Coastal Zones			5a. CONTRACT NUMBER		
			5b. GRANT NUMBER		
			5c. PROGRAM ELEMENT NUMBER		
6. AUTHOR(S)			5d. PROJECT NUMBER		
			5e. TASK NUMBER		
			5f. WORK UNIT NUMBER		
7. PERFORMING ORGANIZATION NAME(S) AND ADDRESS(ES) Control & Dynamical Systems,,and Environmental Engineering Science, 107-81,,California Institute of Technology,,Pasadena,,CA, 91125			8. PERFORMING ORGANIZATION REPORT NUMBER		
9. SPONSORING/MONITORING AGENCY NAME(S) AND ADDRESS(ES)			10. SPONSOR/MONITOR'S ACRONYM(S)		
			11. SPONSOR/MONITOR'S REPORT NUMBER(S)		
12. DISTRIBUTION/AVAILABILITY STATEMENT Approved for public release; distribution unlimited					
13. SUPPLEMENTARY NOTES					
14. ABSTRACT The goal of this research program is to develop a more detailed and systematic understanding of transport and mixing in the oceans and coastal zones. Ultimately, the program will lead to Lagrangian forecasting, that is, the ability to make specific deterministic predictions about the advection and diffusion of passive scalars in the ocean. To accomplish this, it will be necessary to unify several rapidly advancing areas: aspects of dynamical systems theory developed to identify transport barriers and coherent Lagrangian structures, Lagrangian stochastic models of turbulent diffusion, and Eulerian observation data, e.g. sea surface height (SSH) from the TOPEX/Poseidon altimeter for global/regional studies and high frequency (HF) radar for coastal studies.					
15. SUBJECT TERMS					
16. SECURITY CLASSIFICATION OF:			17. LIMITATION OF ABSTRACT Same as Report (SAR)	18. NUMBER OF PAGES 20	19a. NAME OF RESPONSIBLE PERSON
a. REPORT unclassified	b. ABSTRACT unclassified	c. THIS PAGE unclassified			

understanding and predicting how currents influence anything that is drifting in the ocean, from passive contaminants to an underwater glider.

APPROACH

The study of transport and mixing in fluids problems has long been approached from a Eulerian perspective, i.e. observing quantities such as velocity and concentration of scalar material, such as a contaminant in a bay, as it moves past a stationary reference frame. The evolution of velocity and concentration in a Eulerian reference frame are described by the advection-diffusion equation. The problem with this equation is that it contains nonlinear advection terms and so when applied to a turbulent flow, the evolution equations for the mean velocity and mean concentration are not closed. In other words, they involve higher order statistics such as the Reynolds stresses and scalar density fluxes. Closure approximations introduced to overcome this problem depend on the concentration field itself, and so are not uniformly valid. The other alternative is to observe the flow from a Lagrangian perspective, tagging individual particles and noting the property changes that each particle experiences. A Lagrangian perspective allows the flow and concentration to be described in a reference frame that follows a point moving with the fluid. The primary advantage of using a Lagrangian framework is that the time derivative following the motion includes the nonlinear advection terms implicitly. The analog of the advection-diffusion equation in a Lagrangian framework is thus trivial, stating that a fluid particle retains its original concentration as it moves through the fluid. Since a particle conserves its concentration, changes in the concentration field occur solely due to redistribution throughout the fluid. The closure problem still remains, but approximations now only involve the velocity field and not the concentration field. In addition to this theoretical advantage, a Lagrangian approach, i.e. a particle tracking approach does not require the solution of an additional partial differential equation and is thus computationally more efficient. Our approach uses dynamical systems theory to analyze and understand the deterministic, albeit chaotic advection of scalars, while using Lagrangian stochastic models to determine the effect of turbulent diffusion.

During the second year of this program, the key individuals in this study include Francois Lekien at Caltech, George Haller at the Massachusetts Institute of Technology, Andy Reynolds at the Silsoe Research Institute, Arthur Mariano at the University of Miami, Jeff Paduan at the Naval Post-graduate School, the PI and co-PI, Chad Coulliette and Jerrold Marsden, respectively.

WORK COMPLETED

Our progress this year toward accomplishing our Lagrangian forecasting goals was divided into three subject areas. The first subject area was the application and use of criteria-based invariant manifold approximation methods, such as direct finite-time Lyapunov exponents, to unfiltered HF radar data from both Monterey Bay and the east coast of Florida. We use the manifold approximations to demonstrate by example that it is possible to use unfiltered HF radar data to predict the optimal time to release contaminants into the coastal zone. The second subject area is the development of an Open-boundary Model Analysis (OMA) to filter HF radar velocity data and other oceanographic measurement data when some or all of the boundaries are open, i.e. there is flow across some of the boundaries. OMA represents a significant improvement over previous modal projection filtering methods. It projects data onto both closed and open boundary modes and uses an unstructured mesh, yielding more accurate solutions and allowing for a more accurate representation of the boundary, respectively. The last subject area is the development of a Lagrangian stochastic (random flight)

model for the purpose of understanding the relationship between coherent Lagrangian structures and turbulent diffusion. Typically, the influence of eddies and other Eulerian flow structures beneath the resolved length scale of the ocean model or measurements on Lagrangian trajectories and identified structures are either ignored, or treated simplistically through a Langevin equation, which typically assumes that the unresolved turbulence is homogeneous. However, it is contradictory to assume homogeneous turbulence in the vicinity of identified Lagrangian structure. Thus, we developed a Lagrangian stochastic model capable of demonstrating the effect of inhomogeneous turbulence on parcel trajectories and Lagrangian structures. Our new approach described in this report successfully circumvents both of these limitations. We have encoded our new approach into a software package called MANGEN, which includes a graphical user interface. MANGEN runs on a variety of different operating systems, including Windows, Linux, and any UNIX system. However, at this time the graphical user interface is compatible only with the Windows platforms. We are in the process of porting the graphical user interface to a wide variety of UNIX/Linux platforms.

RESULTS

The release of pollution in coastal areas can lead to dramatic consequences for local ecosystems if the pollutants recirculate close to the coast rather than being transported out to the open ocean and safely absorbed. Using a combination of accurate current measurements and recent developments in nonlinear dynamical systems theory, we uncover previously unknown flow structures that govern mesoscale ocean mixing. More specifically, the flow structures we refer to are Lagrangian structures, i.e., structures that move with the fluid. Knowledge of these Lagrangian structures will lead to predictions on a number of phenomena, ranging from the motion of plankton populations to the evolution of oil spills. We demonstrate how Lagrangian structures can be exploited to reduce the damaging effects of coastal pollution. In contrast to earlier approaches to optimal pollution release in simple flow models, we rely on real-time data obtained directly from coastal radar antennas.

We examine high-frequency (HF) radar measurements of near-surface currents in Monterey Bay. The temporal complexity of these currents becomes evident from tracking different evolutions of a fluid parcel--a model for a blob of contaminant-- released at the same precise location, but at slightly different times. We show the results of two such numerical experiments in Fig. 1. Note that the black contaminant parcel remains in the bay, whereas the white parcel clears from the Bay and moves towards the open ocean. The latter scenario is highly desirable, because it minimizes the impact of the contaminant on coastal waters, by causing it to be safely dispersed in the open ocean. This observation inspires us to understand and predict different evolution patterns of the same fluid parcel, depending on its initial location and time of release.

A recently developed nonlinear technique, the Direct finite-time Lyapunov Exponent (DLE) analysis, identifies repelling material in flow data as local maximizing curves of material stretching. Composed of fluid particles, these curves remain hidden to naked-eye observations of unsteady current plots, yet turn out to fully govern global mixing patterns in the fluid. Such Lagrangian structures in measured ocean data have previously been inaccessible to analysis for lack of an efficient extraction method. The DLE algorithm starts with the computation of the flow map, the map that takes an initial fluid particle position \mathbf{x}_0 at time t_0 to its later position $\mathbf{x}(t, \mathbf{x}_0)$ at time t . We then compute the largest singular value of the spatial gradient of the flow map. More specifically, we compute a scalar field $\sigma_1(\mathbf{x}_0, t_0)$ as

the largest eigenvalue of the Cauchy-Green strain tensor $\left[\partial \mathbf{x}(t, \mathbf{x}_0) / \partial \mathbf{x}_0 \right]^T \left[\partial \mathbf{x}(t, \mathbf{x}_0) / \partial \mathbf{x}_0 \right]$, with the

superscript T referring to the transpose of a matrix. Repelling material lines are local maximizing curves or ridges of the scalar field $\sigma_t(\mathbf{x}_0, t_0)$. The same procedure performed backward in time (i.e., for $t < t_0$) would render attracting material lines at t_0 as ridges of $\sigma_t(\mathbf{x}_0, t_0)$.

Using DLE analysis, however, we have found a highly convoluted repelling material line (superimposed on snapshots of parcel positions on Fig. 1) that acts as a barrier between two different kinds of motion: re-circulation and escape from the bay. We call this barrier a Lagrangian coherent structure (LCS).

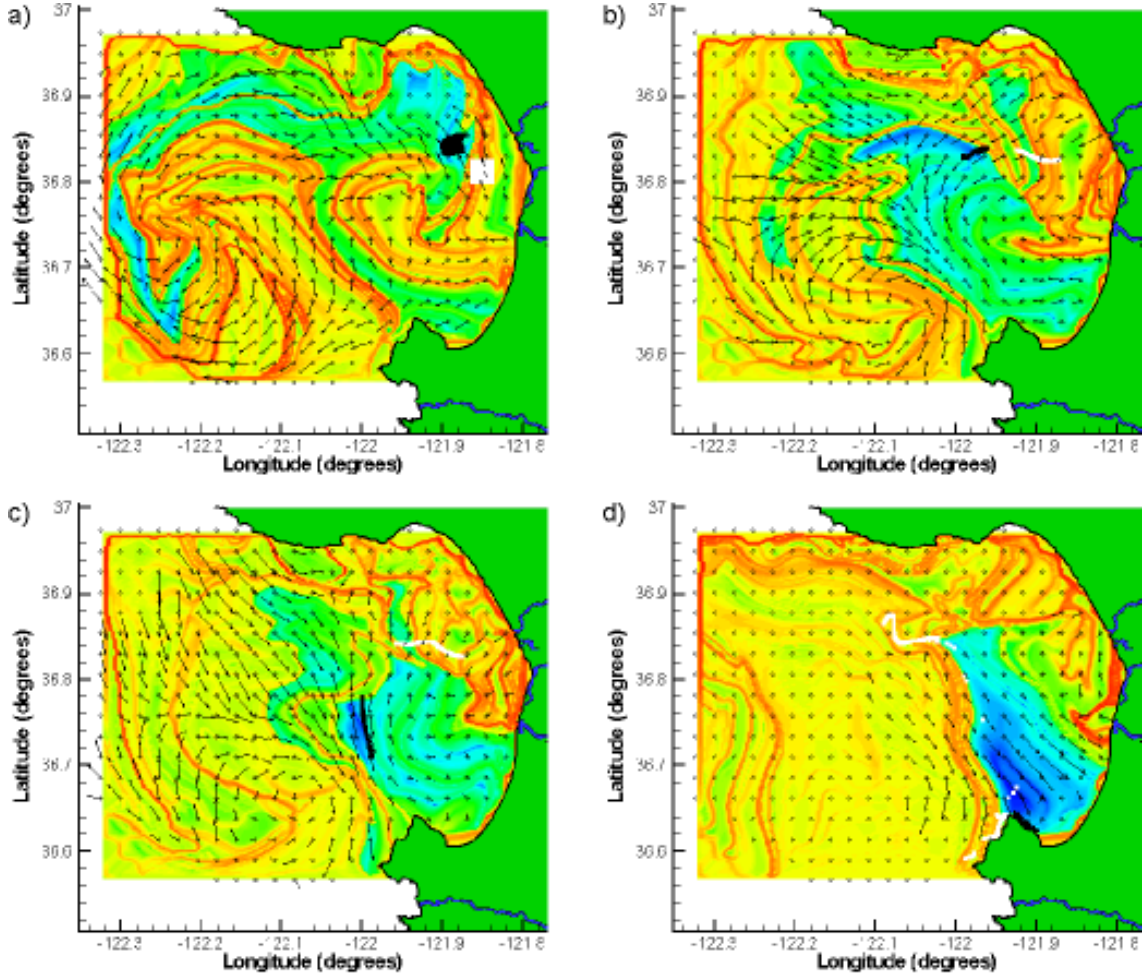


Figure 1. Two parcels of contaminants released from the same position near Moss Landing at 22:00 GMT, August 6, 2000 (black) and at 09:00 GMT, August 7, 2000 (white). The black parcel remains in the bay, while the white parcel departs from the bay. The black arrows show instantaneous surface velocities captured by the HF radars. The ridges of the DLE field reveal the hidden Lagrangian structure of the bay at the same time instants. The two parcels are released on different side of the barrier line, explaining their different behaviors.

We are primary interested in the behavior and predictive qualities of a particular LCS which is attached to the coastline near Point Pinos, as shown in Fig. 1. If we follow this particular LCS from

Point Pinos, it first travels north-east from the point, then in a meandering, albeit clockwise manner around the perimeter of the bay, passing Santa Cruz and then Moss Landing. It is the meandering of this LCS in the vicinity of Moss Landing which is most interesting and useful. Fluid parcels in the region near Moss Landing that are located to the west of the LCS will re-circulate in the bay after they pass by the coastal attachment point of LCS at Point Pinos, and most likely continue to circulate for much longer. However, parcels located to the east of the LCS efficiently exit to the open ocean after passing by the attachment at Point Pinos. This explains the different parcel behaviors we observed in Fig. 1: a parcel released at the exact same location, but at slightly different times of on August 6 and August 7 of 2000, ended up on opposite sides of this particular LCS.

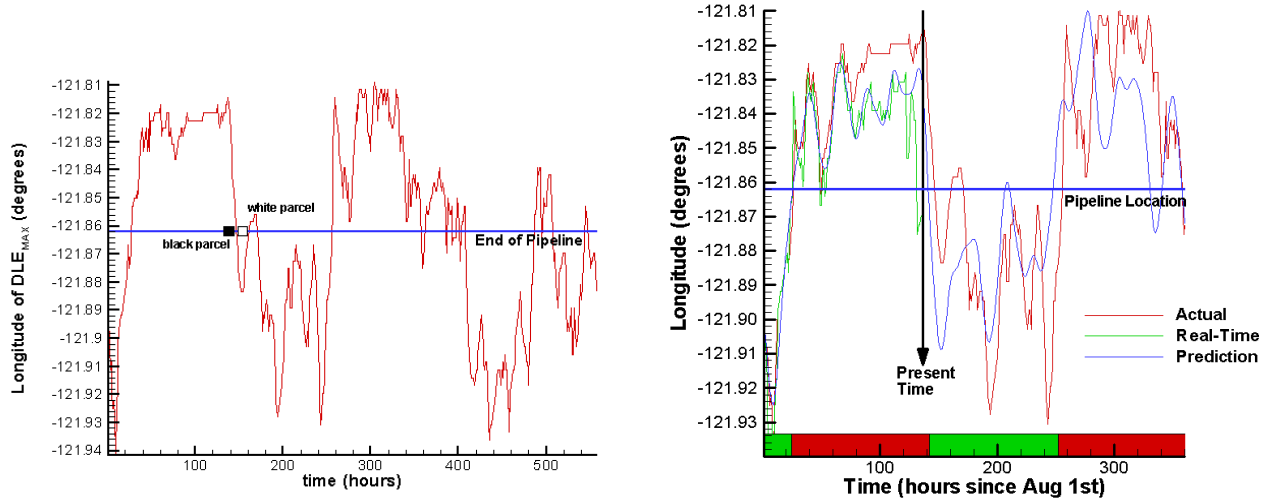


Figure 2. Left Panel: Longitudinal oscillation of the barrier point in front of Moss Landing. The zero reference time corresponds to 07:00 GMT, August 1, 2000. The horizontal line marks the longitude of the release location. The black and white squares represent the release time and longitude of the parcels featured in Fig. 1. Right Panel: Actual, real-time and predicted barrier point location along the longitude of the release point. The colored bar at the bottom of the figure indicates the periods of desirable releases (green) and the periods to avoid (red). The prediction is relative to the simulated “present time” of 22:00 GMT, August 6, 2000. Note that no data after the present time was used to make the prediction.

Based on the above analysis, we propose a pollution release scheme that minimizes the effect of contaminants on the coast of Monterey Bay. Although building a pipeline is not essential to our method, to expedite our explanation we will imagine a pipeline which carries the contaminants from the Moss Landing area to an offshore release site at the same location that the black and white parcels were released. For any given time, we consider a portion of the previously discussed LCS as it descends along the coastline of the bay from Santa Cruz, meandering southward past Moss Landing. The meandering of the LCS may cause it to intersect the axis of our pipeline in several points. We refer to the first such intersection point—measured along the LCS its coastal attachment point—as the barrier point.

According to the above discussion, if the barrier point is east of the pipeline outlet, between the outlet and the coast, then the pollution released from the outlet will re-circulate in the bay. However, if the barrier point falls west of the pipeline outlet, such that the pipeline outlet is between the LCS and the coastline, the pollution released will exit the bay without re-circulating. Obviously, the latter scenario is most desirable, since the contaminants can be more safely absorbed in this manner.

The motion of the barrier point along the axis of the pipeline is complicated, as evidenced by the left panel of Fig. 2. Superimposed on this plot are the release time and release location of the white and black parcels of Fig. 1. The white parcel exits the bay quickly because it is released when the red curve is below the blue horizontal line, i.e., the pipeline outlet lies between the barrier point and the coastline.

Using maximum entropy transforms, we have identified the main frequency components of the barrier point motion. Surprisingly, the most influential component of this motion is not the tidal oscillation (with a period of 24 hours), but rather a component with a period of 8.6 days. To minimize the effect of coastal pollution, we propose using a holding tank that stores contaminants produced during a typical 5 day period. The tank is used to store pollution during the half-period of the barrier point in which it would be disadvantageous to release the contaminants. The contents of the tank are released once the barrier point is on west side of the pipeline outlet. Perhaps contrary to expectations, pollution release tied to high tide is typically not optimal: the dominant frequency in the oscillation of the barrier point lies far from frequencies associated with the tidal oscillation and its subharmonics.

To use our algorithm, we propose a prediction based on the motion of the Lagrangian structures (as opposed to Eulerian velocities). We chose Aug 6, 2000 22:00 GMT as the present time and computed the DLE plots (shown in Fig. 1) and the barrier point using only data up to the present time. The resulting “real-time” barrier curve is shown in the right panel of Fig. 2. We used all the significant frequencies of the spectrum of this curve to predict the barrier point location along the axis of the pipeline in the near future. The right panel of Fig. 2 shows the predicted barrier point together with the actual and the real-time locations. Note how faithfully the predicted curve reproduces the main features of the actual DLE peak oscillations. From this prediction, we determined environmentally friendly future time windows. These windows last for about 100 hours, over which most of the pollution released from the pipeline will advect towards the open ocean. A general physical lesson from our analysis is that focused Lagrangian predictions for a geophysical flow (such as the prediction of material barrier locations) can be feasible even if global Eulerian (i.e., velocity based) predictions are unrealistic.

We also did a similar study on data from the east coast of Florida in cooperation with Arthur Mariano. An OSCAR VHF model was deployed for the Southern Florida Ocean Measurement Center (SFOMC) 4-Dimensional Current Experiment from June 25-August 25, 1999 by Shay, Mariano and Ryan. Radio waves are backscattered from the moving ocean surface by surface waves of one-half of the incident radar wavelength. This Bragg scattering effect (Stewart 1974) results in two discrete peaks in the Doppler spectrum. In the absence of surface current, spectral peaks are symmetric and their frequencies are offset from the origin by an amount proportional to the surface wave phase speed and the radar wavelength. If there is an underlying surface current, Bragg peaks in the Doppler spectrum are displaced by the radial component of current along the radar's look direction. Using two radar stations sequentially transmitting radio waves resolves the two-dimensional velocity vector for placing the data into a geophysical context. The two transmit/receive stations operated at 50 MHz and sent

electromagnetic signals scattered from surface gravity waves with 3-m wavelengths. Coastal ocean currents were mapped over a 7 km by 8.5 km domain at 20 minute intervals with a resolution of 250 m. The radars were located in John Lloyd State Park, Dania Beach (Master) and an oceanfront site in Hollywood Beach (Slave) which equated to a distance of 7 km.

Contour level sets of the Lyapunov exponents are shown in Fig.3. During the two months of the experiment, the plot reveals a strong stable Lagrangian barrier, i.e., repelling material line, attached to the coast near Fort Lauderdale, propagating to the southeast. This repelling material line acts as a Lagrangian barrier between the coastal recirculating zone (southwest of the material line) and the Florida Current (northeast of the same material line). The material line is a barrier in the sense that particles cannot cross it. Superimposed on Fig.3. are two typical parcels. A quick analysis reveals that any particle northeast of the barrier (white parcel) is flushed out of the domain in only a few hours. In contrast, parcels starting southwest of the barrier (black parcel) typically re-circulate several times near the Florida coast before they can finally rejoin the current. A corresponding animation can be downloaded at <http://transport.caltech.edu/florida.html>. It is important to realize that without the use of DLE or a similar criteria-based method, the Lagrangian structures would still be there, but could not be seen or made use of in this way. We prefer to think of the currents as not influencing particle paths directly, but rather that the currents influence the Lagrangian structure, such as causing transport barriers and alleyways, and the Lagrangian structures influence the particle paths.

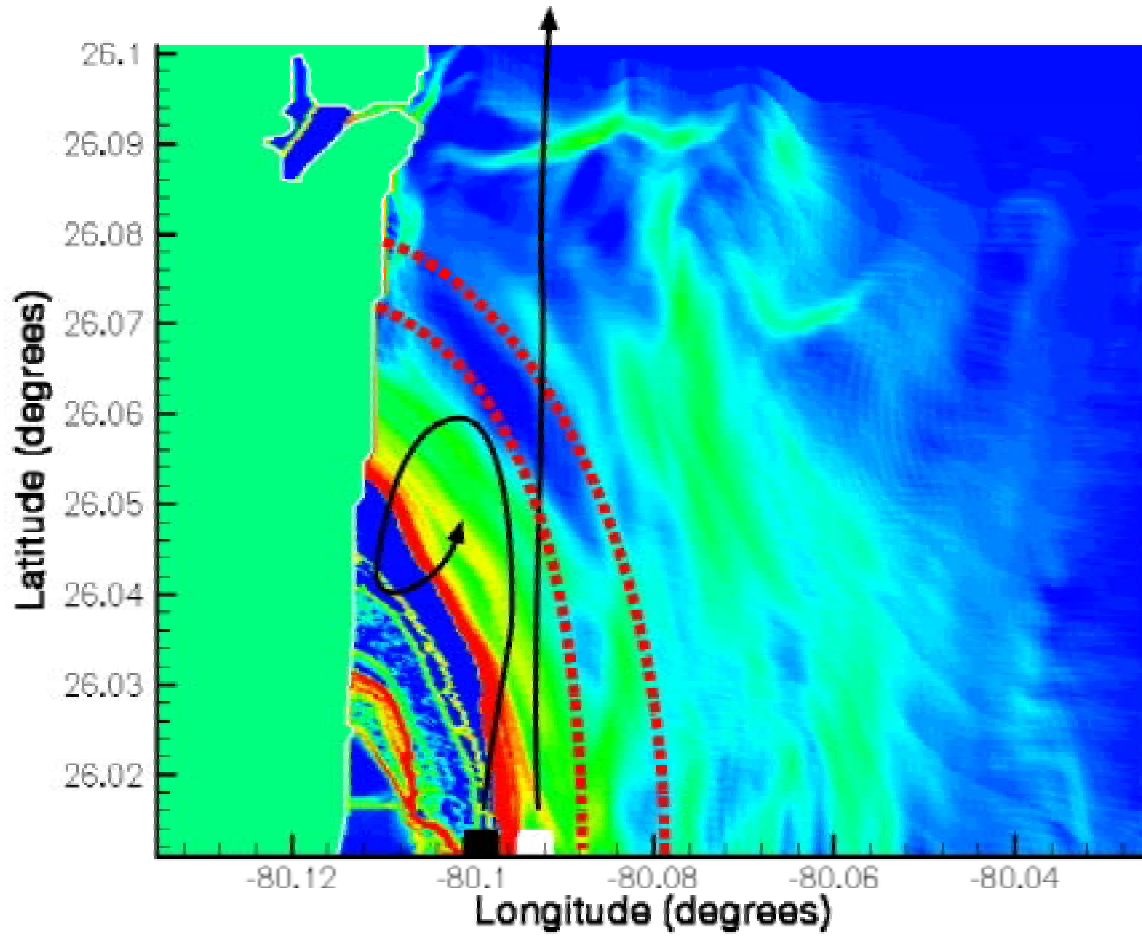


Figure 3. *Contour level sets of finite-time Lyapunov exponents computed from HF radar data on the east coast of Florida. During the two months of the experiment, the plot reveals a Lagrangian barrier, indicative of a stable manifold, attached to the coast near Fort Lauderdale and propagating to the southeast. Particles cannot cross this barrier, so it divides trajectories into two qualitatively distinct regions, a coastal recirculating zone (southwest of the material line) and the Florida Current (northeast of the same material line). The red dashed curves indicate future shapes and oscillations of the Lagrangian barrier. Superimposed are two typical parcels and their corresponding trajectories. The black parcel will re-circulate near the coast for a long time, while the white parcel escapes to the north, leaving the domain.*

We remark that the location of the base of the repelling material line (on the coast) can be used as a criteria to minimize the effect of coastal pollution. We will refer to the intersection of the coastline and the repelling material line as the barrier point. Factories and sewing centers along the coast should not release anything if the barrier point is located North of them. To illustrate how an efficient pollution release algorithm can be set up, we imagined a source of pollution with a fixed position along the coast. Using the DLE contours, which change as a function of time, we identify zones of (green)

favorable release (when the invariant manifold is below the position of the factory) and (red) dangerous release (when the invariant manifold is above the factory).

To minimize the effect of coastal pollution, we propose using a holding tank that stores contaminants during dangerous release zones. The tank stores pollution during the half-period of the DLE barrier point oscillation, during which contaminants should not be released. The contents of the tank are released once the barrier point passes south of the pollution source. Shown in Fig.4 is the total mass of contaminants for the two release mode. Clearly, by using information from the DLE plots, the white factory (dashed curve) is able to reduce by a factor of three (area under the curves) the local contamination caused by the same amount of pollution.

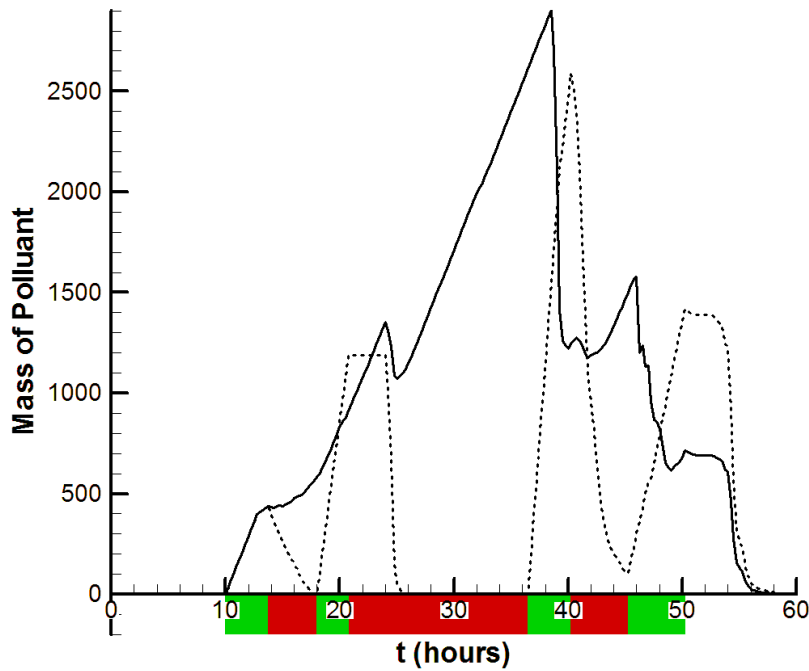


Figure 4. *The total mass of pollutants present in the region of study as a function of time. The green and red zones beneath the horizontal axis are the optimal and non-optimal release times predicted by the movement of the DLE barrier point, respectively. The black curve represents the total mass of pollutants when the amount released does not vary as a function of time. The dashed curve represents the total mass when pollution is only released during the green optimal-release time periods.*

We have shown the existence of a set of repelling material lines in radar data obtained from the Fort Lauderdale area on the Florida coast. We have also shown how these material lines can be used to minimize the effect of coastal pollution by determining optimal release times. This approach can be used for making predictions about the trajectories of buoyant contaminants or the trajectories of nearly Lagrangian tracers. The data source can be VHF radar data or any other current data source, such as data-assimilated ocean models that approximate the near-surface velocity field to some reasonable

level of accuracy. The other advantage of using ocean models is that the velocity provided is 3D+1, thus we can explore the Lagrangian structures that develop at various depths. We could either compute horizontal slices of the manifolds at various depths by initializing the DLE algorithm with trajectories at a given depth and then allowing the 3D+1 model to advect the trajectories to any 3D position, or we could compute and visualize the entire set of invariant manifolds by initializing the trajectories for the DLE algorithm everywhere in the domain. The former would be easier to inspect, but the latter would provide more complete information about the chaotic stirring and transport processes of the flow that is modeled. Since three-dimensional models are becoming more readily available and configured for various areas, we are currently in the process of extending MANGEN to compute finite-time Lyapunov exponents, other criteria-based field approximations, and the SP-HT approach for 3D+1 velocity data. A real-time experimental realization to test the accuracy of our prediction abilities and pollution release is important, but cannot be performed until funding is available to release large quantities of GPS-equipped Lagrangian drifters while simultaneously collecting HF radar surface velocity data and ADCP data from various depths. In this test, we could compute invariant unstable and stable manifolds using finite-time Lyapunov exponents or a similar approach from an ocean model which has assimilated all of the HF radar and ADCP data, then we could compare the trajectories of the GPS-equipped drifters with the transport barriers and avenues indicated by the invariant manifolds. This would yield a statistical estimate for the accuracy of this approach.

Rather than using the unfiltered HF radar velocity data as in the above examples, or assimilating the unfiltered HF radar velocity data into an ocean model, we can instead use a basis of functions to filter, extrapolate and interpolate the data. Significant effort has been made in the past to use a basis of functions for these objectives. However, none of the past approaches have allowed the freedom of unknown boundary conditions on segments of open boundaries (such as the west side of the Monterey Bay domain shown in Fig. 1). Fig. 5 depicts such a situation, where Ω is the domain, $\partial\Omega$ is the boundary of the domain, and is made of two different segments of boundary. $\partial\Omega_0$ is the closed portion of the boundary and corresponds to an actual segment of the coastline. We will typically enforce slip or no-slip boundary conditions on $\partial\Omega_0$. The remainder of the boundary, $\partial\Omega_1$, is not a coastline and no assumptions should be made about the flow in this region. The main improvement introduced by OMA is to let the user select the boundary conditions on $\partial\Omega_0$ whilst the portion $\partial\Omega_1$ is determined during the data projection. The HF radar data in the domain Ω and the modes are used to determine the velocity on $\partial\Omega_1$, such as having all in flow, all out flow, or a partially in flow and partially out flow.

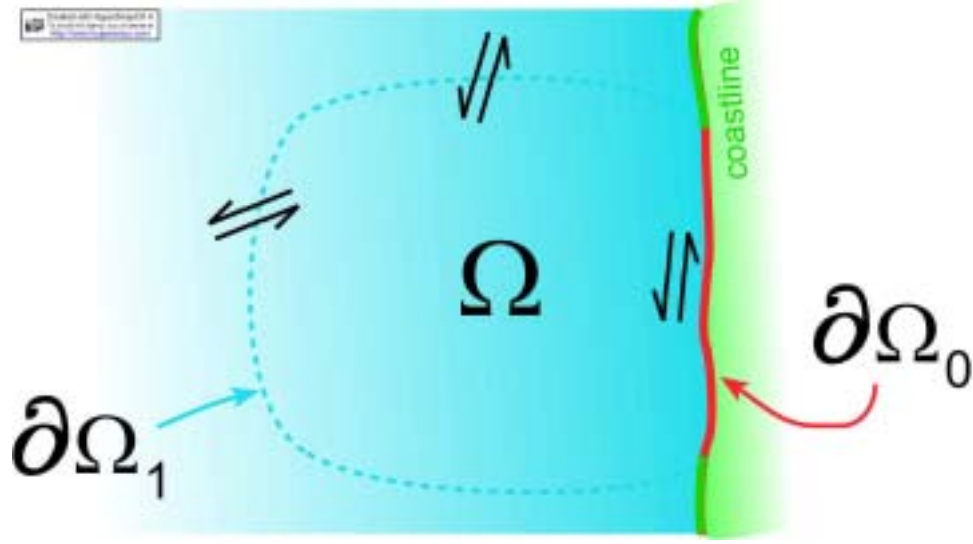


Figure 5. Schematic of the domain for using Open-boundary Modal Analysis (OMA). Ω is the domain, $\partial\Omega$ is the boundary of the domain, and is made of $\partial\Omega_0$ (the closed portion of the boundary) and $\partial\Omega_1$ (open portion of the boundary). Note that OMA works in the limit that entire boundary is either open or closed. In fact, the latter limit reduces OMA to other many of the other approaches that only work properly with closed boundaries.

Mathematically speaking, we derived a function basis in Sobolev spaces W^1 and W^1_0 that satisfy the boundary conditions (Neumann or Dirichlet) on the segment of closed boundaries, yet do not prescribe any velocity on the open boundary. The projection of the HF radar data on the mode is solely responsible for the numerical value of the velocity and the flux across the open boundary. The general decomposition for the nowcast velocity is given by

$$u = \sum_i u_i^{\psi} + \sum_i u_i^{\phi},$$

where u_i^{ψ} are incompressible modes and u_i^{ϕ} are irrotational modes. Separating the modes incompressible and irrotational is convenient for many types of studies, such as determining the effects of upwelling and downwelling. The sequence of modes that we chose is complete in the subset of W^1 , thus representing all possible velocity fields in the domain of interest. If we were using all the modes, the error would be zero, but that would require an infinite number of measurements to determine the infinite numbers of coefficients. Instead we will assume that only a finite number of modes are computed. That means that we arbitrarily set the other coefficients, i.e. that we project the real velocity in a subspace of the space of all available W^1 velocities that are tangent to the coastline. The choice of the modes and in particular the number of modes used is a key concept of the filtering. Using less (low energy) modes results in a velocity field far away from the HF radar data but with very simple features. An example of the 2nd incompressible mode solved on an unstructured grid is shown in Figure 6. Note that only a single mode captures the double gyre pattern often observed in the HF radar data of Monterey Bay. In contrast, if too many modes are used, the solution matches the HF radar data, but does not sufficiently filter and smooth the data.

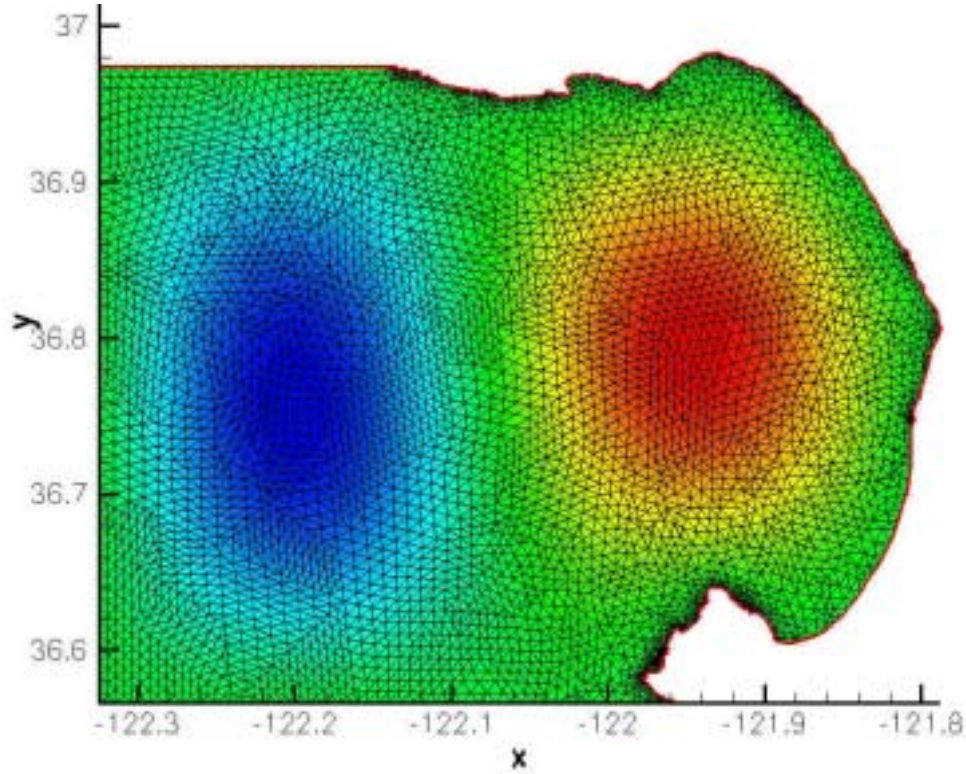


Figure 6. An example of the 2nd incompressible mode solved on an unstructured (finite-element type) grid. An unstructured grid is able to adapt to a complex coastline, unlike the limitation of the staircase coastline caused by other modal filtering methods. The size and shape of each triangular element is solution adaptive, chosen by the numerical method to optimize the accuracy of the mode geometry. It is trivial to interpolate to a Cartesian grid afterward, if that is useful for the application, which yields higher accuracy than solving directly on a Cartesian grid.

We project the HF radar data in a typical manner, by minimizing the distance between the measurements and the value computed using the nowcast velocity. Another option is less typical, to try to minimize the error on the Lagrangian Coherent Structure (LCS) that we are computing. Using a criteria linking the error on LCS with the error on the Eulerian vector field, we modified the function to be minimized (or equivalently the norm of the Sobolev space) to produce velocity field nowcasts that are optimized for Lagrangian analysis. Note that only a brief review of OMA has been provided in this report since the corresponding paper (Lekien & Coulliette 2002) has not been accepted for publication yet.

Similar to that shown in Fig. 6, many applications from the fluid dynamics laboratory to oceanographic flows, computer modeling or observational data typically results in a discretized velocity field. Whether the grid used is Cartesian, orthonormal, or unstructured (as with OMA described above), the knowledge we have of the flow under study is limited by the spacing between grid points in space and time. In a laminar flow, this limited knowledge may be adequate to sufficiently describe how particles are advected through this flow. But, in a turbulent flow, we need a way to determine the effect of the ‘sub-grid’ scale, below which structure is not resolved, on particle trajectories. Attempts have been made to model the unresolved Lagrangian dynamics as an Ornstein-Uhlenbeck process by assuming

homogeneity and stationarity of the velocity statistics at the sub-grid scale. We overcome this limitation through the employment of a more sophisticated Lagrangian stochastic model capable of capturing inhomogeneous and unsteady effects.

There are two possible approaches to modeling transport in fluids: the Eulerian one in which material transport in a stationary frame of reference is considered; and the Lagrangian one in which the trajectories of marked particles is considered. Of the two, the Lagrangian one is the more natural and has the advantage of implicitly incorporating the non-linear advection term and of being valid at times less than the integral Lagrangian timescale. These models require Eulerian velocity statistics as inputs. Observations and modeling cannot capture all the scales of fluid motion with the consequence that some scales, the ‘sub-grid’ scales of motions, will not be resolved and so represented explicitly in the data for \mathbf{u} . It is, for example, computationally prohibitive to resolve all of the spatial-temporal scales of a turbulent flow in numerical simulations of geophysical or environmental problems. This limitation can be circumvented by Reynolds-averaging of the Navier-Stokes equations or by applying a spatial-temporal filter to the Navier-Stokes equations. The former approach provides predictions for the moments of the velocity distribution whilst the later, which treats explicitly the larger-slower scales of motion, can capture coherent structures. Similarly, instrument response time and the finite size of sampling volumes result in a filtering of observational data and a loss of resolution at smaller-faster scales. Filtering also arises as a consequence of the discrete sampling of the velocity field and when the smoothing is applied to reduce instrument or numerical noise.

Several attempts have been made to model the unresolved Lagrangian stochastic motions as an Ornstein-Uhlenbeck process by assuming homogeneity and stationarity of the sub-grid scales of motion. This assumption is incompatible with the occurrence of inhomogeneity and nonstationarity at the resolved scales of motion. This is because flow structures occurring at different spatial-temporal scales are coupled through the turbulent cascade process, with the transfer rate and statistical properties of the smaller-eddies being dependent upon the slowest and largest structures in the cascade. A proper account of the role played by the sub-grid scales of motion in turbulent dispersion in inhomogeneous flows therefore requires the adoption of more sophisticated Lagrangian stochastic (LS) models that are consistent with inhomogeneous non-stationary turbulence at sub-grid scales. Apart from providing more accurate predictions for dispersion and a self-consistent framework for study of turbulent dispersion in the presence of coherent structures, such models may also provide a means for the schematic incorporation of turbulent velocity fluctuations in the dynamical systems picture of dispersion. The formulation of a LS model for inhomogeneous non-stationary turbulence at the sub-grid scales along with the parameterization of the distribution of sub-grid scale turbulent velocity fluctuations, required as the model input, are described next. Application of this approach to an idealized flow and its use in conjunction with observation data for a bay and data from a quasi-geostrophic model of the ocean follow afterward.

For sufficiently large Reynolds numbers the acceleration autocorrelation function approaches a delta function at the origin corresponding to an uncorrelated component velocity. In this limit it is, therefore, appropriate to assume that the position, \mathbf{x} , and velocity, \mathbf{u} , of a tracer-particle evolve jointly as a Markov process. We determined the form of the deterministic functions of the model using the well-mixed condition which currently constitutes the most rigorous correct mathematical framework for the formulation of LS models. Mathematically, the well-mixed condition requires solving the Fokker-Planck equation Eulerian probability density function for fluid velocities, $P_E(\mathbf{x}, \mathbf{u}, t)$,

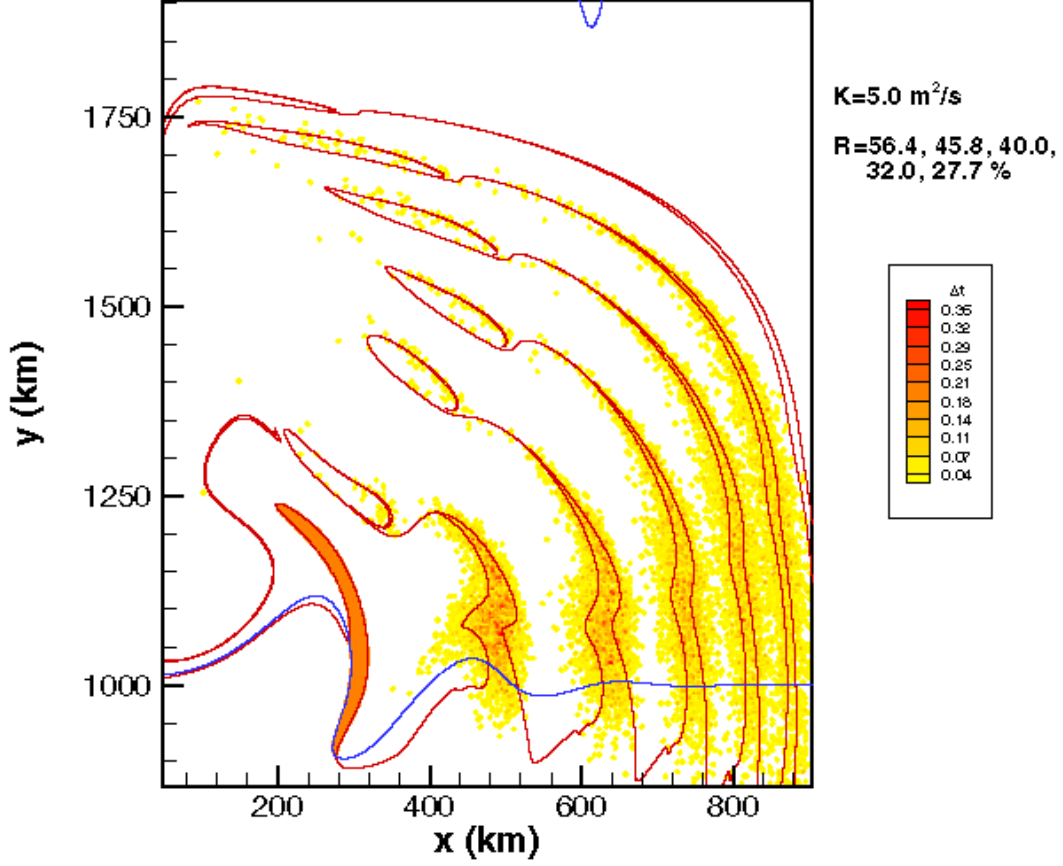


Figure 7. Application of this LS model to the Lagrangian coherent structures described by intersections of invariant stable and unstable manifold in the upper layer of a three-layer quasigeostrophic model. The color spectrum represents a probability distribution function for the geometry of the coherent structures.

$$\frac{\partial P_E}{\partial t} + \frac{\partial(u_i P_E)}{\partial x_i} = -\frac{\partial(a_i P_E)}{\partial u_i} + \frac{1}{2} C_0 \epsilon \frac{\partial^2 P_E}{\partial^2 u_i}. \quad (2)$$

The variance of the applied stochastic velocity field, is a key parameter in any LS model. In Eulerian models it can be calculated using an explicit form of sub-grid model, if available, but generally can be estimated from the spectral density function $E(k)$, which is the contribution to the fluid turbulent kinetic energy from velocity fluctuations with wave-numbers having a magnitude between k and $k+dk$. The precise form for $E(k)$ is not known but at wave-numbers associated with the production of turbulent kinetic energy, $E(k) \propto k^4$ whilst at wavenumbers associated with the inertial subrange, $E(k) = C_k \epsilon^{2/3} k^{-5/3}$ where $C_k = 1.5$. The invoking of Kolmogorov's similarity theory is appropriate here because all the criteria for the establishment of an inertial subrange are satisfied by oceanic and atmospheric turbulence. Note, however, that it is not necessary for the sub-grid scales to lie entirely within the inertial subrange. Here, in common with many studies of dispersion in atmospheric

turbulence, the form of the spectra at intermediate wavenumbers is approximated by the von Karman form,

$$E(k) = \frac{C_k \varepsilon^{2/3} k^4}{(\zeta + k^2)^{17/6}} \quad (6)$$

which provides a differentiable interpolation between the k^4 and $k^{-5/3}$ regimes. The parameter ξ is determined by Eqn. 4, i.e. by equating the resolved turbulent energy with the integral of $E(k)$ from $k=0$ to $k=k_c$. The solution to Eqn. 4 for ξ was performed with the aid of tabulation (i.e with the use look-up tables indexed by $^{1/2}\langle U^2 \rangle / \varepsilon^{2/3}$) and interpolation rather than by iteration, which proved to be computationally much less efficient. This difficulty arises because the integral is non-analytic and can be circumvented at the expense of accuracy by adopting a simplified form for $E(k)$ (Appendix A). However, such an approach is not readily extended to unsteady turbulence. For unsteady turbulence, it is assumed that the energy at each wavenumber is spread over a range of frequencies (with variance σ_ω^2) around a characteristic frequency $\langle \omega \rangle$ in a Gaussian distribution so that,

$$E(k, \omega) = E(k) \frac{\exp(-(\omega - \langle \omega \rangle)^2 / 2\sigma_\omega^2(k))}{(2\pi)^{1/2} \sigma_\omega(k)} \quad (7)$$

where $\omega' = \omega - \langle \omega \rangle$. For inertial subrange turbulence, $\langle \omega \rangle$ and σ_ω^2 are determined by Kolmogorov's similarity theory, i.e. $\langle \omega \rangle = \sigma_\omega = \varepsilon^{1/3} k^{2/3}$, but for more general cases, their specification becomes problematic. Here, for simplicity inertial subrange scaling is adopted irrespective of the observed scaling at a given wavenumber, k .

The validity of the sub-grid LS model has been examined. We were able to show that the approach is exactly correct, in the sense of reproducing the exact equations of motion, when the turbulence is isotropic and homogeneous. More generally, the approach has the advantage over previous ones of being consistent with inhomogeneous and non-stationary Eulerian velocity statistics at the sub-grid scale. This allows for self-consistent numerical simulations of dispersion in complex flow situations, an example of which is shown in Figure 7: we applied this LS model to the Lagrangian coherent structures described by intersections of invariant stable and unstable manifold in the upper layer of a three-layer quasigeostrophic model. The red curve is the unstable manifold, which originates near a hyperbolic trajectory on the western boundary, near the stagnation point between the northern and southern gyres. The blue curve is the stable manifold, which attaches to the hyperbolic trajectory on the eastern boundary. The intersection of the manifolds identify regions which in dynamical systems theory are called lobes. From a more physical point of view, the lobes are coherent Lagrangian regions. Unfortunately, in a quasigeostrophic ocean model, it is necessary to parameterize the effect of smaller scales through an eddy viscosity. By using a Lagrangian stochastic model in this context, we can account for the diffusive effects of the parameterized scales on Lagrangian trajectories and structures. Note that the color spectrum represents a probability distribution function for the geometry of the coherent structures. So, from this simulation, it is easy to see the effect of turbulent diffusion. Many opponents of the dynamical systems approach to identifying Lagrangian structure have claimed that turbulent diffusion would make such identification useless. But, in this simulation we have set the turbulent diffusivity equal in magnitude to the eddy viscosity, so that we have closure, but the diffusion is quite reasonable, even for structures that have advected across the entire width of the basin. The geometry of the Lagrangian structures remains intact, and even the shape of the ring is still identifiable after being advected and diffused over a significant distance and time. Note that only the

key ideas of our LS model have been presented here. Some of the details were intentionally not discussed here since these results are very recent and thus the corresponding paper has not been accepted for publication yet.

IMPACT/APPLICATIONS

There is a tremendous potential impact for this study in any area where it is desirable to predict where any passive tracer will drift. We have specifically shown by example how this newly developed approach could be used to predict if contaminants released in a bay will be advected quickly from the bay or remain in the bay indefinitely. Although there are many laws in our country that specify how contamination must be treated chemically before being released into our coastal zone, there are not any laws (to our knowledge) specifying precisely when contaminants can be released. This is because up until now it has been thought that predicting where contaminants in a bay, estuary or other coastal zones will be advected is impossible. Perhaps lawmakers can use the information about this new approach described in this report to regulate more precisely when contaminants can be released in our coastal zone. In addition, there are many other possible applications of this approach. We could use a similar approach to predict where oil spills will be advected, to determine more exactly how currents alter the trajectory of drogues or underwater gliders, or possibly to reduce the search area for persons that have fallen overboard from a vessel at sea.

TRANSITIONS

Several research groups at universities throughout the world have requested copies of our MANGEN software. Many requests for MANGEN were made when we attended the General Assembly of the European Geophysical Society in Nice, the 7th Experimental Chaos Conference in San Diego, hosted by the American Institute of Physics, and the International Conference on Mathematical Geophysics in Torin, Italy.

RELATED PROJECTS

Recent progress in nonlinear dynamical systems has revealed the fundamental role of Lagrangian coherent structures in fluid transport. While several algorithms exist for the extraction of such structures from numerical flow models, the relationship between model Lagrangian structures and their counterparts in the true flow (if any) has remained unclear. Recent work by George Haller (Massachusetts Institute of Technology) has revealed that Lagrangian coherent structures found in model data tend to give accurate predictions for similar flow structures in the real flow. This work was in part inspired by this program at Caltech to interpret Lagrangian predictions obtained from HF radar data. An ongoing effort is to use Haller's results in deriving error bars on Lagrangian predictions for Monterey Bay. We have been testing our advances in dynamical systems theory to find Lagrangian structures on HF radar data of Monterey Bay, collected by Jeff Paduan, from the Naval Post-graduate school. To verify the generality of our approach, we have also tested finite-time Lyapunov exponents and other criteria-based approaches on HF radar data from the east coast of Florida collected by Arthur Mariano at the University of Miami. We are also working with Naomi Leonard and her group at Princeton on the AOSN2 project. In particular, we are aiding in the development of the control laws for the underwater gliders used for adaptive sampling. The gliders will use groups of three gliders to gradient-climb scalar fields, such as temperature, or possibly a criteria-based field approximation of the unstable or stable invariant manifolds. By gradient climbing a criteria-based approximation, the

underwater gliders can use invariant manifolds as efficient avenues to travel from their insertion point to the area where adaptive sampling is needed. Another interesting use of finite-time Lyapunov exponents and other similar criterion is to evaluate the sum of the measured velocity field and the control law of the gliders. Instead of the manifolds representing Lagrangian barriers for passive particle advection, they would represent barriers to the abilities of the gliders in that particular flow with that particular control law. Thus, the presence of several manifolds in the Lyapunov exponent field would indicate the gliders will have difficulty reaching many locations within the region of study. A lack of manifolds in the field demonstrates the efficiency of that particular control law, i.e. that the gliders will be able to travel to nearly any location within the area of study without difficulty.

REFERENCES

1. Prahl, F. G., Crecellus, E. & Carpenter, R. Polycyclic aromatic hydrocarbons in Washington coastal sediments: an evaluation of atmospheric and riverine routes of introduction. *Environ Sci Technol* **18**, 687-693 (1984).
2. Rice, D. W., Seltenrich, C. P., Spies, R. B. & Keller, M. L. Seasonal and annual distribution of organic contaminants in marine sediments from the Elkhorn Slough, Moss Landing Harbor and nearshore Monterey Bay, California. *Environmental Pollution* **82**, 79--91 (1993).
3. Verschueren, K. *Handbook of Environmental Data on Organic Chemicals* (Van Nostrand Reinhold Co., New York, 1983).
4. Paduan, J. D. & Rosenfeld, L. K. Remotely sensed surface currents in Monterey Bay from shore-based HF radar (CODAR). *J. Geophys. Res.* **101**, 20669--20686 (1996).
5. Paduan, J. D. & Cook, M. S. Mapping surface currents in Monterey Bay with CODAR-type HR radar. *Oceanography* **10**, 49--52 (1997).
6. Prandle, D. & Ryder, D. K. Measurement of surface currents in Liverpool Bay by high-frequency radar. *Nature* **315**, 128 - 131 (1985).
7. Goldstein, R. M. & Zebker, H. A. Interferometric radar measurement of ocean surface currents. *Nature* **328**, 707 - 709 (1987).
8. Georges, T. M., Harlan, J. A. & Lematta, R. A. Large-scale mapping of ocean surface currents with dual over-the-horizon radars. *Nature* **379**, 434-436 (1996).
9. Webb, T. & Tomlinson, R. B. Design procedures for effluent discharge into estuaries during ebb tide. *J Envir Engrg* **118**, 338-362 (1992).
10. Smith, R. Optimal use of holding tanks to avoid pollution in narrow estuaries. *IMA J Appl Math* **51**, 187-199 (1993).
11. Smith, R. Using small holding tanks to reduce pollution in narrow estuaries. *Journal of Hydraulic Engineering* **124**, 117--122 (1998).

12. Kay, A. Advection-diffusion in reversing and oscillating flows. 1: The effect of a single reversal. *IMA J Appl Math* **45**, 115-137 (1990).
13. Gould, D. J. & Munro, D. in *Coastal discharges* 45-50 (Thomas Telford, London, U.K., 1981).
14. Giles, R. T. Optimal strategies for discharging pollutants into narrow estuaries. *Water Res* **29** (1995).
15. Bikangaga, J. H. & Nussehi, V. Application of computer modeling techniques to the determination of optimal effluent discharge policies in tidal water systems. *Water Res* **29**, 2367-2375 (1995).
16. Stirling, J. R. Transport and bifurcation in a non-area-preserving two-dimensional map with applications to the discharge of pollution in an estuarine flow. *Physica D* **144**, 1-2 (2000).
17. Haller, G. Finding finite-time invariant manifolds in two-dimensional velocity fields. *Chaos* **10**, 99-108 (2000).
18. Haller, G. & Yuan, G. Lagrangian coherent structures and mixing in two-dimensional turbulence. *Physica D* **147**, 3-4 (2000).
19. Haller, G. Distinguished material surfaces and coherent structures in 3D fluid flows. *Accepted*. (2001).
20. Fischer, H. B., Brooks, N. H., Imberger, J., Koh, R. C. Y. & List, E. J. Mixing in inland and coastal waters. (1979).
21. Watson, A. J., Messias, M. J., Fogelqvist, E., Scoy, K. A. V. & et.al. Mixing and convection in the Greenland Sea from a tracer-release experiment. *Nature* **401**, 902 - 904 (1999).
22. Zimmerman, J. T. F. The tidal whirlpool--- a review of horizontal dispersion by tidal and residual currents. *Netherlands J. Sea Res.* **20**, 133--154 (1986).
23. Ridderinkhof, H. & Zimmerman, J. T. F. Chaotic stirring in a tidal system. *Science* **258**, 1107--1111 (1992).
24. Ridderinkhof, H., Zimmerman, J. T. F. & Philippart, M. E. Tidal exchange between the North-Sea and Dutch Walden Sea and mixing time scales of the tidal basins. *Netherlands J. Sea Res.* **25**, 331--350 (1990).
25. Pasmanter, R. Physical Processes in Estuaries. 42--52 (1988).
26. Beerens, S. P., Ridderinkhof, H. & Zimmerman, J. T. F. Longitudinal dispersion in natural streams. *Chaos, Solitons and Fractals* **4**, 1011--1029 (1998).
27. Lekien, F. & Coulliette, C. MANGEN: Computation of Hyperbolic Trajectories, Invariant Manifolds and Lobes of Dynamical Systems Defined as 2D+1 Data Sets. *In Progress* (2001).

PUBLICATIONS

Coulliette, C., Lekien, F., Haller, G., Marsden, J., and Paduan, J.D., “Optimal Pollution Release in Monterey Bay Based on a Nonlinear Analysis of Coastal Radar Data”, Submitted to *Physical Review Letter* (2002).

Coulliette, C., Lekien, F., Haller, G., Marsden, J., and Paduan, J.D., “Lagrangian structures in HF radar data of Monterey Bay as revealed by finite-time Lyapunov exponents, with application to optimal pollution release times”, Submitted to *Journal of Physical Oceanography* (2002).

Coulliette, C. and Reynolds, A.M., “A Lagrangian stochastic model for dispersion in unsteady inhomogeneous sub-grid scale turbulence”, Submitted to *Journal of Fluid Mechanics* (2002).

Coulliette, C. and Wiggins, S., “Intergyre transport in a wind-driven, quasigeostrophic double gyre: An Application of Lobe Dynamics” (black & white printing) *Nonlinear Processes in Geophysics*, **7**(1), 59-86 (2000).

Coulliette, C. and Wiggins, S., “Intergyre transport in a wind-driven, quasigeostrophic double gyre: An Application of Lobe Dynamics” (color printing) *Nonlinear Processes in Geophysics*, **8**(1/2), 69-94 (2001).

Lekien, F., and Coulliette, C., “Open-boundary Modal Analysis (OMA): Function basis for domains with flow across the boundary and a practical projection method for interpolation, extrapolation and filtering”, Submitted to *Physics of Fluids* (2002).

Lekien, F., Coulliette, C., and Marsden, J., “Lagrangian Structures in Very High-Frequency Radar Data and Optimal Pollution Timing”, Proceedings of the 7th Experimental Chaos Conference, American Institute of Physics, San Diego, CA; Accepted for publication on August (2002), to be published in March (2003).

Lekien, F., and Coulliette, C., “Dynamical systems analysis of transport in geophysical flows”, International Conference on Mathematical Geophysics, Torin, Italy, June 20 (2002).

Lekien, F., and Coulliette, C., “MANGEN: Computation of Hyperbolic Trajectories, Invariant Manifolds and Lobes of Dynamical Systems Defined as 2D+1 Data Sets”, European Geophysical Society General Assembly, Nice, March (2001).

Lekien, F., and Coulliette, C., “Dynamical systems analysis of flows defined as data sets: contaminant control on the coast of Florida”, European Geophysical Society General Assembly, April 25 (2002).

PATENTS

MANGEN software (2001-2002).